nature portfolio

https://doi.org/10.1038/s41586-022-05588-y

Supplementary information

Structure-based design of bitopic ligands for the μ-opioid receptor

In the format provided by the authors and unedited

Supporting Information For:

Structure-based design of functionally selective bitopic ligands for the μ-opioid receptor

Abdelfattah Faouzi[1+], Haoqing Wang[2+], Saheem A. Zaidi[3+], Jeffrey F. DiBerto[4+], Tao Che[1,4+], Qianhui Qu[2,5+], Michael J. Robertson[2,5], Manish K. Madasu[1], Amal El Daibani[1], Balazs R. Varga[1], Tiffany Zhang[6], Claudia Ruiz,[8] Shan Liu,[7] Jin Xu,[7] Kevin Appourchaux[1], Samuel T. Slocum[4], Shainnel O. Eans[9], Michael D Cameron, Ream Al-Hasani[1],Ying Xian Pan[6,7], Bryan L. Roth[4], Jay P. McLaughlin[9], Georgios Skiniotis[2,5]*, Vsevolod Katritch[3]*, Brian K. Kobilka[2]* and Susruta Majumdar[1]*.

[1]Center for Clinical Pharmacology, University of Health Sciences & Pharmacy and Washington University School of Medicine, St. Louis, MO 63131, USA.
[2]Department of Molecular and Cellular Physiology, Stanford University School of Medicine, 279 Campus Drive, Stanford, CA 94305, USA.
[3]Department of Quantitative and Computational Biology; Department of Chemistry; Bridge Institute; Michelson Center for Convergent Bioscience, University of Southern California, Los Angeles, CA 90089, USA.
[4] Department of Pharmacology, University of North Carolina School of Medicine, Chapel Hill, NC 27599, USA.
[5] Department of Structural Biology, Stanford University School of Medicine, 279 Campus Drive, Stanford, CA 94305, USA.
[6]Department of Neurology and Molecular Pharmacology, Memorial Sloan Kettering Cancer Center, New York, NY 10065, USA.
[7]Department of Anesthesiology, Rutgers New Jersey Medical School, Newark, NJ 07101, USA.
[8] Department of Chemistry, Scripps Research, Jupiter, Florida 33458, United States.
[9]Department of Pharmacodynamics, University of Florida, Gainesville, FL 32610, USA.

[+] AF, HW, SAZ, TC, JFD and QQ contributed equally

Corresponding author(s)

*Georgios Skiniotis PhD
Email: yiorgo@stanford.edu

*Vsevolod Katritch PhD
Email: Katritch@usc.edu

*Brian Kobilka MD, PhD
Email:kobilka@stanford.edu

and

*Susruta Majumdar PhD
Email: susrutam@email.wustl.edu

Table of Contents:

S1: Material and Methods Section

Drugs and Materials.

Opiates were provided by the Research Technology Branch of the National Institute on Drug Abuse (Rockville, MD). **C5-guano** and all new compounds were synthesized as described later on in the text. [^{125}I]IBNtxA were synthesized at MSKCC as previously described.[1,2] Na^{125}I was purchased from Perkin-Elmer (Waltham, MA). Miscellaneous chemicals and buffers were purchased from Sigma-Aldrich.

Chemistry

Reagents purchased from Sigma-Aldrich Chemicals, Fisher scientific, Alfa Aesar; were used without further purification. While performing synthesis, reaction mixtures were purified by silica gel flash chromatography on E. Merck 230–400 mesh silica gel 60 using a Teledyne ISCO CombiFlash R_f instrument with UV detection at 280 and 254 nm. RediSep R_f silica gel normal phase columns were used with a gradient range of 0–10% MeOH in DCM. Reported yields are isolated yields upon purification of each intermediate. Final clean (purity ≥95%, LC-MS Agilent 1100 Series LC/MSD) compounds were used for the study. NMR spectra were collected using Varian 400 MHz NMR instrument at the NMR facility of Washington University School of Medicine in St. Louis collected via the Bruker Topspin Software (Bruker Topspin 3.5 pI 6). Chemical shifts are reported in parts per million (ppm) relative to residual solvent peaks at the nearest 0.01 for proton and 0.1 for carbon ($CDCl_3$ ^{1}H: 7.26, ^{13}C: 77.1; and CD_3OD ^{1}H: 3.31, ^{13}C: 49.0). Peak multiplicity is reported as the NMR spectra were processed with MestreNova software14.2.0, namely s – singlet, d – doublet, t – triplet, q – quartet, m – multiplet for examples. Coupling constant (*J*) values are expressed in Hz. Mass spectra were obtained at the St. Louis

College of Pharmacy using the Agilent 1100 Series LC/MSD by electrospray (ESI) ionization with a gradient elution program (Ascentis Express Peptide C18 column, acetonitrile/water 5/95/95/5, 5 min, 0.05% formic acid) and UV detection (214 nM/254 nM). High resolution mass spectra were obtained using a Bruker 10 T APEX -Qe FTICR-MS and the accurate masses are reported for the molecular ion $[M+H]^+$. Detail experiments and characterization of the new compounds are included in the supporting information section.

Radioligand Competition Binding Assays in opioid Receptor

[^{125}I]IBNtxA binding was carried out in membranes prepared from Chinese Hamster Ovary (CHO) cells stably expressing clones of μOR as previously described.[1,2] Binding incubations were performed at 25 °C for 90 min in 50 mM potassium phosphate buffer, pH 7.4, containing 5 mM magnesium sulfate. After the incubation, the reaction was filtered through glass-fiber filters (Whatman Schleicher & Schuell, Keene, NH) and washed three times with 3 mL of ice-cold 50 mM Tris-HCl, pH 7.4, on a semiautomatic cell harvester. Nonspecific binding was defined by addition of levallorphan (8 μM) to matching samples and was subtracted from total binding to yield specific binding. K_i values were calculated by nonlinear regression analysis (GraphPad Prism, San Diego, CA). Protein concentrations were determined using the Lowry method with BSA as the standard.

For species comparisons, [^{3}H]DAMGO binding was carried out in membranes prepared from HEK293T cells transiently expressing human or mouse μOR. Binding incubations were performed at 25 °C for 90 min in 50 mM TRIS hydrochloride buffer, pH 7.4, containing 10 mM magnesium chloride and 0.1 mM EDTA. After the incubation, the reaction was filtered through Unifilter 96 GF/C PEI coated microplates (PerkinElmer) and washed three times with 3 mL of ice-cold 50 mM

Tris-HCl, pH 7.4, via vacuum filtration on cell harvester. Nonspecific binding was defined by addition of naloxone (10 μM) to matching samples and was subtracted from total binding to yield specific binding. Ki values were calculated by nonlinear regression analysis (GraphPad Prism, San Diego, CA). Protein concentrations were determined using the BCA assay with BSA as the standard.

cAMP inhibition assay[3]

To measure μOR Gi-mediated cAMP inhibition, HEK293T (ATCC CRL-11268) cells were co-transfected with human μOR along with a luciferase-based cAMP biosensor (GloSensor; Promega) and assays were performed similar to previously described. After 16 h, transfected cells were plated into Poly-lysine coated 384-well white clear bottom cell culture plates with DMEM + 1% dialysed FBS at a density of 15,000-20,000 cells per 40 mL per well and incubated at 37ºC with 5% CO_2 overnight. The next day, drug solutions were prepared in fresh drug buffer [20 mM HEPES, 1X HBSS, 0.3% bovine serum album (BSA), pH 7.4] at 3X drug concentration. Plates were decanted and received 20 mL per well of drug buffer (20 mM HEPES, 1X HBSS) followed by addition of 10 mL of drug solution (3 wells per condition) for 15 min in the dark at room temperature. To stimulate endogenous cAMP via β-adrenergic-Gs activation, 10 mL luciferin (4 mM final concentration) supplemented with isoproterenol (400 nM final con- centration) were added per well. Cells were again incubated in the dark at room temperature for 15 min, and luminescence intensity was quantified using a Wallac TriLux microbeta (Perkin Elmer) luminescence counter. Results (relative luminescence units) were plotted as a function of drug concentration, normalized to % DAMGO, U50,488h or DPDPE stimulation, and analyzed using ‘‘log(agonist) vs. response’’ in GraphPad Prism 8.0.

Tango arrestin recruitment assay

The μOR Tango constructs were designed and assays were performed as previously described. HTLA cells expressing TEV fused-β-Arrestin2 were transfected with the μOR Tango construct. The next day, cells were plated in DMEM supplemented with 1% dialyzed FBS in poly-L-lysine coated 384-well white clear bottom cell culture plates at a density of 10,000-15,000 cells/well in a total of 40 ml. The cells were incubated for at least 6 h before receiving drug stimulation. Drug solutions were prepared in drug buffer (20 mM HEPES, 1X HBSS, 0.3% BSA, pH 7.4) at 3X and added to cells (20 ml per well) for overnight incubation. Drug solutions used for the Tango assay were exactly the same as used for the cAMP assay. The next day, media and drug solutions were removed and 20 ml per well of BrightGlo reagent (purchased from Promega, after 1:20 dilution) was added. The plate was incubated for 20 min at room temperature in the dark before being counted using a luminescence counter. Results (relative luminescence units) were plotted as a function of drug concentration, normalized to % agonist control stimulation, and analyzed using ‘‘log(agonist) vs. response’’ in GraphPad Prism 8.0.

BRET based assays (TRUPATH and arrestin signaling)[4–6]

Cells were plated either in 6-well dishes at a density of 700,000–800,000 cells per well, or 10 cm dishes at 7–8 million cells per dish. Cells were transfected 2–4 h later, using a 1:1:1:1 DNA ratio of receptor:Gα-RLuc8:Gβ:Gγ-GFP2 (100 ng per construct for 6-well dishes, 750 ng per construct for 10 cm dishes), except for the Gγ-GFP2 screen, where an ethanol coprecipitated mixture of Gβ1–4 was used at twice its normal ratio (1:1:2:1). Transit 2020 (Mirus Biosciences) was used to complex the DNA at a ratio of 3 μl Transit per μg DNA, in OptiMEM (Gibco-ThermoFisher) at a concentration of 10 ng DNA per μl OptiMEM. The next day, cells were harvested from the plate

using Versene (0.1 M PBS + 0.5 mM EDTA, pH 7.4) and plated in polyD-lysine-coated white, clear-bottom 96-well assay plates (Greiner Bio-One) at a density of 30,000–50,000 cells per well. One day after plating in 96-well assay plates, white backings (PerkinElmer) were applied to the plate bottoms, and growth medium was carefully aspirated and replaced immediately with 60 µl of assay buffer (1× Hank's balanced salt solution available under aCC-BY-NC-ND 4.0 International license. was not certified by peer review) is the author/funder, who has granted bioRxiv a license to display the preprint in perpetuity. It is made bioRxiv preprint doi: https://doi.org/10.1101/2021.04.22.440994; this version posted May 7, 2021. The copyright holder for this preprint (which (HBSS) + 20 mM HEPES, pH 7.4), followed by a 10 µl addition of freshly prepared 50 µM coelenterazine 400a (Nanolight Technologies). After a 5 min equilibration period, cells were treated with 30 µl of drug for an additional 5 min. Plates were then read in an LB940 Mithras plate reader (Berthold Technologies) with 395 nm (RLuc8-coelenterazine 400a) and 510 nm (GFP2) emission filters, at integration times of 1 s per well. Plates were read serially six times, and measurements from the sixth read were used in all analyses. BRET2 ratios were computed as the ratio of the GFP2 emission to RLuc8 emission.

Expression and purification of µOR

In this study, we used a mouse µOR construct with cleavable N- and C-terminal domains as described previously.[7] Basically, Mouse full-length MOR with N-terminal hemagglutinin (HA) signal sequence and FLAG tag, and C-terminal histidine tag was expressed in *Spodoptera frugiperda* Sf9 insect cells using the baculovirus method (Expression Systems). The receptors were extracted from insect cell membranes with 1% *n*-dodecyl-β-D-maltoside (DDM, Anatrace)/0.1% cholesterol hemisuccinate (CHS), and purified by nickel-chelating sepharose chromatography.

The Ni-NTA eluate in DDM was then incubated with 1% lauryl maltose neopentyl glycol (L-MNG)/0.1% CHS for 1 hour on ice to exchange the detergents. After detergent exchange, 2mM $CaCl_2$ was added and the sample was loaded onto M1 anti-Flag resin and washed with progressively lower concentrations of salt and naloxone. The μOR was then eluted from M1 resin in a buffer consisting of 20 mM Hepes pH 7.5, 100 mM NaCl, 0.003% L-MNG/0.0003% CHS supplemented with 1 uM naloxone, Flag peptide and 5 mM EDTA. The M1 elute was further purified by size exclusion chromatography on the Superdex 200 10/300 gel filtration column (GE Healthcare) in 20 mM HEPES pH 7.5, 100 mM NaCl, 0.003% L-MNG/0.0003% CHS. The monomeric fractions were pooled, concentrated, and flash frozen in liquid nitrogen.

Expression and purification of heterotrimeric G_i

Heterotrimeric G_i was expressed and purified as previously described.[8] Basically, *Trichuplusia ni* Hi5 insect cells were co-infected with two viruses, one encoding the wild-type human Gαi subunit and another encoding the wild-type human β1γ2 subunits with an histidine tag inserted at the N-terminus of the β1 subunit. After 48 hours, cells were harvested and lysed in hypotonic buffer. The heterotrimeric Gi was extracted in a buffer containing 1% sodium cholate and 0.05% DDM. The soluble fraction was purified using Ni-NTA chromatography, and the detergent was exchanged from cholate/DDM to DDM on column. After elution, human rhinovirus 3C protease (3C protease) was added and the histidine tag was cleaved overnight at 4°C during dialysis. Then the heterotrimeric Gi without tag will be further purified through reverse Ni-NTA chromatography. Finally, the flow through of the reverse Ni-NTA step will be purified by the Mono Q 5/50 GL column (GE Healthcare) to get rid of the 3C protease. The purified heterotrimeric G_i will be

concentrated, stored in 20 mM HEPES pH 7.5, 100 mM NaCl, 0.05% DDM, 100 uM TCEP, 10 uM GDP before complexing.

Expression and Purification of scFv16

scFv16 was developed and purified as previously described.[9,10] Basically, scFv with C terminal His tag was expressed in *Trichuplusia ni Hi5* insect cells. After infection and expression, the insect cell supernatant was loaded onto Ni-NTA resin and the scFv was eluted in 20 mM HEPES pH 7.5, 500 mM NaCl, and 250 mM imidazole. The eluate was incubated with 3C protease overnight to cleave the C-terminal His tag. After dialysis into the buffer consisting of 20mM HEPES pH 7.5 and 100 mM NaCl, scFv16 was further purified by reverse Ni-NTA chromatography. The flow-through was collected and applied over a Superdex 200 16/60 column (GE Healthcare). The scFv16 fractions were pooled, concentrated, and flash frozen.

Formation and purification of the μOR–Gi-scFv16 complex.

500uM bitopic ligands (C5 guano, C6 guano) was added to purified μOR while 1% L-MNG was added to purified $G_{i.}$ Both mixtures were incubated on ice for 1 h. After that, ligand-bound μOR was mixed with a 1.5 molar excess of Gi heterotrimer and extra TCEP was added to maintain 100uM TCEP concentration. The coupling reaction was allowed to proceed for another 1 h on ice, followed by addition of apyrase to catalyze GDP hydrolysis to obtain nucleotide free complex. After 30min, a 2 molar excess of scFv16 was also added. The reaction mixture was left on ice overnight to allow stable complex formation. After that, the complexing mixture was purified by M1 anti-Flag affinity chromatography and eluted in 20 mM Hepes pH 7.5, 100 mM NaCl, 0.003% L-MNG, 0.001% glyco-diosgenin (GDN), 0.0004% CHS, 10 uM bitopic ligand, 5 mM EDTA and

Flag peptide. After elution, 100uM TCEP was added to provide a reducing environment. Finally, the μOR–Gi-scFv16 complex was purified by size exclusion chromatography on a Superdex 200 10/300 gel filtration column in 20 mM Hepes pH 7.5, 100 mM NaCl, 5 uM bitopic ligand, 0.003% L-MNG and 0.001% GDN with 0.0004% CHS total. Peak fractions were concentrated to ~10 mg/ml for electron microscopy studies.

Cryo-EM sample preparation and image acquisition

For cryo-EM, 3 μL sample was directly applied to glow-discharged 300 mesh gold grids (Quantifoil R1.2/1.3) and vitrified using a FEI Vitrobot Mark IV (Thermo Fisher Scientific). For C5-guano bound μOR–Gi-scFv16 complex, movies were collected on a Titan Krios (Stanford cEMc) operated at 300 keV using a Gatan K2 Summit direct electron detector in counting mode, with 1.06 Å pixel size. A total of 3470 movies were obtained. Each stack movie was recorded for a total of 10 s with 0.2 s per frame. The dose rate was 1.34 electrons/$Å^2$/subframe, resulting in an accumulated dose of 67 electrons per $Å^2$ (**Extended Data Figure 2A**). For C6 guano bound μOR–Gi-scFv16 complex, movies were collected on a Titan Krios (SLAC/Stanford) operated at 300 keV using a Gatan K3 direct electron detector in counting mode, with 0.4338 Å pixel size. A total of 3019 movies were obtained. Each stack movie was recorded for a total of 2.5 s with 0.05 s per frame. The dose rate was 1.37 electrons/$Å^2$/subframe, resulting in an accumulated dose of 68.5 electrons per $Å^2$ (**Extended Data Figure 2B**). Both datasets were collected using SerialEM. [11]

Cryo-EM data processing

Dose-fractionated movies were subjected to beam-induced motion correction using RELION3.[12] For the C5-guano bound μOR–Gi-scFv16 dataset, we used unbinned movie while for the C6-guano

bound μOR–Gi-scFv16 dataset, the movies were binned by 2, resulting in 0.8676 Å pixel size. CTF parameters for each micrograph were determined by CTFFIND-4.1.[13] Particle autopicking, 2D and 3D classification, and 3D auto-refine were performed in RELION3. Briefly, autopicked particles were first subjected to 2D classification (**Extended Data Figure 2**), and particles in 2D classes showing all features of a GPCR-G protein complex were selected for 3D classification (**Extended Data Figure 2**). The cryo-EM map of DAMGO bound μOR-Gi-scFv16 complex was low-pass filtered to 60Å and used as reference for 3D classification. After that, the best 3D class (highest estimated resolution and highest class distribution) was selected and the particles subjected to 3D auto-refine. Further CTF refinement and Bayesian polishing of these particles were performed in RELION3 as well, followed by another round of 3D classification without image alignment and with T=40. The highest estimated resolution 3D classes were then selected and refined. This generated a 3.2Å resolution map for C5-guano bound μOR–Gi-scFv16 complex and a 3.3Å resolution map for C6-guano bound μOR–Gi-scFv16 complex (**Extended Data Figure 2-3**).

To improve the local resolution of the receptor in the cryoEM map, we also performed density subtraction, in which scFv16 and detergent micelle densities were subtracted. This improved the receptor local resolution for C6-guano bound μOR–Gi-scFv16 dataset (**Extended Data Figure2B**, **Extended Data Figure3B**) but not the C5guano bound μOR–Gi-scFv16 dataset (data not shown). Local resolution estimation was also performed in RELION3.

Model building and refinement

Ligand models and restraints were generated by eLBOW in Phenix1.19.2.[14] Models were first docked into the cryo-EM map in Chimera1.17,[15] followed by iterative manual adjustment in

COOT0.9.3,[16] and real space refinement in Phenix1.19.2. Ligand coordination were also optimized by GemSpot-Maestro 2021-4.[17] The refinement statistics were provided in **Extended Data Table 2**.

Molecular Docking. The receptor proteins were extracted from the RCSB server for mouse μOR (PDBID: 5c1m), representing agonist-bound active state of the receptors. The flexible N-terminal tail of the receptor was removed up to residue Met65, thus removing con-canonical residue YCM57 introduced for covalent binding of BU72. Removal of this flexible N-terminal part is justified by the fact that it is not resolved in other published inactive (4DKL) or active (6DDF and 6DDE) structures of μOR, nor in the cryo-EM structures in this study. All the objects except the receptor protein subunit, the crystallized ligand, and three crystallographic waters important for ligand interactions were deleted from the μOR structure, and the protein was prepared by addition and optimization of hydrogens and optimization of the side chain residues. Ligands were sketched, assigned formal charges and energy-optimized prior to docking. The ligand docking box for potential grid docking was defined as the whole extracellular half of the protein, and all-atom docking was performed using the energy minimized structures for all ligands with a thoroughness value of 10. The best-scored docking poses, were further optimized by several rounds of minimization and Monte Carlo sampling of the ligand conformation, including the surrounding side-chain residues (within 5 A° of the ligand) and the three crystallographic water molecules in the orthosteric sites. These docking studies were then later also performed employing 5C guano and 6C guano bound resolved cryoEM structures, which provided initial models for 7C, 9C, and 11C guano bound μOR MDs. All the above molecular modeling operations were performed in ICM-Pro v3.8-5 molecular modeling package.

Molecular dynamics simulation protocols

The molecular dynamics simulation setup for the bitopics bound μOR model was built using CHARMM-GUI web server.[18] The initial structure for C5 guano MD simulation was derived from the corresponding cryo-EM structure. For consistency of initial conformations, the initial C6 guano complex was obtained by docking of the ligand into the structure of μOR defined by the C5 guano complex. The CHARMM General Force Field[14] was used to generate CHARMM topology and parameter files for bitopics. The ligand-bound receptor system was embedded in a lipid bilayer with a POPC/cholesterol ≈ 9:1 ratio and with an area of 80 Å × 80 Å. The system was solvated with explicit TIP3P water molecules, ionized with 0.15 M Na^+ cations, and neutralized with Cl^- ions. The resulting simulation system had a total of ~80,000 atoms and occupied an approximate initial volume of 80 Å × 80 Å × 120 Å. The CHARMM36 force field was employed to perform all-atom MD simulations using the GROMACS software package version 2020.2. Following the initial energy minimization of the water boxed, lipid embedded and ionized bitopics bound μOR system, six short equilibration runs were carried out while gradually decreasing harmonic constraints on lipid and protein heavy atoms for a cumulative run of 15 ns. The particle mesh Ewald algorithm was utilized to calculate long-range electrostatic interactions, and van der Waals interactions were switched off gradually between 10 Å to 12 Å. Periodic boundary conditions were applied to simulation boxes, and simulations were run with integration time step of 2 fs at 310 K. The resulting trajectories from several (10 for 5C guano, and 5 for 6C,) independent 1000ns long production runs were analyzed using in-built GROMACS (2020.2) analysis tools. All MD simulations and analyses were performed using the servers at the High-Performance Computing at University of Southern California.

Mice

Male C57BL/6J mice (24–38 g, 8-12 weeks) were purchased from Jackson Laboratories (Bar Harbor, ME). Male CD1 mice (29-45 g, 8–12 weeks of age) were purchased from Charles River Laboratories (Wilmington, MA). Male MOR KO were bred in the McLaughlin laboratory at University of Florida and used when 8-12 weeks old. Progenitors of the colonies for μOR KO were obtained from Jackson Labs. All mice used throughout the manuscript were opioid naïve. All mice were maintained on a 12 hr light/dark cycle with Purina rodent chow and water available ad libitum and housed in groups of five until testing. These mice were kept at a constant temperature of 22 ± 2 °C, and relative humidity was maintained at 40–50%.

All animal studies reported adhere to the ARRIVE guidelines[19]. All procedures were preapproved by the Institutional Animal Care and Use Committee (University of Florida) and conducted according to the 2011 NIH Guide for the Care and Use of Laboratory Animals.

C57BL/6J mice were used in assays of warm-water tail withdrawal[5,20], locomotor and respiration[5,20], acetic acid writhing[20], and conditioned place preference (CPP)[5,21]. Antinociceptive and anti-allodynic effects were confirmed with CD-1 mice in the formalin inflammatory pain assay and chronic constriction nerve injury assay of neuropathic pain.

Tail-withdrawal assay

The 55°C warm-water tail-withdrawal assay was conducted in mice as a measure of acute thermal antinociception as described previously.[22,23] Briefly, each mouse was tested for baseline tail-withdrawal latency prior to drug administration. Following drug administration, the latency for each mouse to withdraw the tail was measured every 10 min until latency returned to the baseline

value. A maximum response time of 15 s was utilized to prevent tissue damage. If the mouse failed to display a tail-withdrawal response within 15 s, the tail was removed from the water and the animal was assigned a maximal antinociceptive score of 100%. Data are reported as percent antinociception, calculated by the equation: % antinociception = 100 x [(test latency - baseline latency)/ (15 - baseline latency)]. This was utilized to account for innate variability between mice. Compounds were administered either, intracerebroventricularly (icv) and the antinociceptive actions of compounds was assessed at as described previously[16]. To briefly describe icv administration: mice were anesthetized using isoflurane. A small (3 mm) incision was made in the scalp, and the drug (2 µl/mouse) was injected (using a 10 µL Hamilton syringe fitted to a 27-gauge needle) into the right lateral ventricle at the following coordinates: 2 mm caudal to bregma, 2 mm lateral to sagittal suture, and 2 mm in depth.

Acetic Acid Writhing Test

The ability of C6 guano to modulate chemically induced visceral pain was assessed with the use of C57BL/6J mice in the acetic acid writhing assay as previously described[20]. After a 25 min pretreatment (icv) of either the vehicle (50% DMSO:saline), morphine (30 nmol), or C6 guano (100 nmol), a second injection of 0.9% acetic acid (i.p., 0.25 mL per 25 g body wt.) was administered to each mouse. After 5 min, the number of stretches presented in each mouse was counted for 15 min. Although the raw number of stretches counted over this time is reported, antinociception was calculated by the formula:

% antinociception = ([{average stretches in the vehicle group} − {number of stretches in each test mouse}]/[average stretches in vehicle group]) × 100.

Formalin Assay

The effectiveness of the ligand's ability to modulate inflammatory pain was performed with the use of C57BL/6J mice in the formalin assay as previously described[20]. After a 10 min pretreatment (*icv*) of dose of the vehicle (50% DMSO:saline), saline, morphine (100 nmol), or C6 guano (100 nmol), an intraplantar (i.pl.) injection of 5% formalin (2.5 μg in 15 μL) was administered into the right hind paw. Time spent licking the right hind paw was recorded in 5 min intervals for 60 min following injection. The last 55 min of the assessment was used to determine the inflammatory response stimulus. Data were analyzed as the summed duration of licking the hind paw.

Chronic Constriction Injury (CCI)

CD-1 mice anesthetized with isoflurane were subjected to chronic constriction injury (CCI), as described previously[20,24] to induce mechanical allodynia and hyperalgesia. Briefly, after anesthetization, mice were subjected to surgery where an incision was made along the surface of the biceps femoris of the right hind paw.[24] Blunt forceps were used to split the muscle and expose the right sciatic nerve. The tips of the two 0.1–10 μL pipette tips facing opposite directions were passed under the sciatic nerve to allow for the easy passing of two sutures under the nerve, 1 mm apart. The sutures were tied loosely around the nerve and knotted twice, and the skin was closed with two 9 mm skin staples. The mice were allowed to recover 7 days prior to baseline von Frey testing, as described above, to confirm the induction of mechanical allodynia in each mouse. A response to von Frey fibers of lower force, otherwise not observed in naïve mice, was an indication of mechanical allodynia, consistent with the demonstration of neuropathic pain. The mice confirmed as allodynic were then administered (icv) either the controls vehicle (50% DMSO:saline), or the test compound C6 guano (10, 30, or 100 nmol). Each mouse was then tested

for the threshold for mechanical allodynia every 20 min up to 80 min post-treatment with the use of calibrated von Frey filaments as described above, until the threshold that induced paw withdrawal was determined as a measure of nocifensive behavior[24].

Respiratory and locomotor effects

Respiration rates and spontaneous ambulation rates were monitored using the automated, computer-controlled Comprehensive Lab Animal Monitoring System (CLAMS, Columbus Instruments, Columbus, OH) as described previously.[21,24] Awake, freely moving adult male mice (C57BL6/J wild-type, μOR KO) were habituated in closed, sealed individual apparatus cages (23.5 cm x 11/5 cm x 13 cm) for 60 min before testing. A baseline for each animal was obtained over the 60-min period before drug injection, and testing began immediately post-injection. Vehicle, morphine (100 nmol, *icv*), or **C6-guano** (100 or 300 nmol, *icv*) were administered (icv) and five min later mice were confined to the CLAMS testing cages for 200 min. Using a pressure transducer built into the sealed CLAMS cage, the respiration rate (breaths/min) of each occupant mouse was measured. Infrared beams located in the floor measured locomotion as ambulations, from the number of sequential breaks of adjacent beams. Data are expressed as percent of vehicle control response.

Conditioned place preference and aversion

Mice were conditioned with a counterbalanced place conditioning paradigm using similar timing as detailed previously.[5,23] Groups of C57BL/6J mice (n = 18–24) freely explored a three-compartment apparatus for 30 min. The amount of time subjects spent in each compartment was measured over the 30 min testing period. Prior to place conditioning, the animals did not demonstrate significant differences in their time spent exploring the left vs right compartments. During each of the next 2 days, mice were administered vehicle (0.9% saline) and consistently

confined in a randomly assigned outer compartment for 40 min, half of each group in the right chamber, half in the left chamber. Four hours later, mice were administered drugs morphine (30 nmol, icv), U50,488h (100 nmol, icv), **C6-guano** (300 nmol, icv) or vehicle and were placed to the opposite compartment for 40 min. Conditioned place preference or aversion data are presented as the difference in time spent in drug- and vehicle associated chambers.

Chronic Constrictive Nerve Injury/Conditioned Place Preference Operant Model of Pain (CCI/CPP)

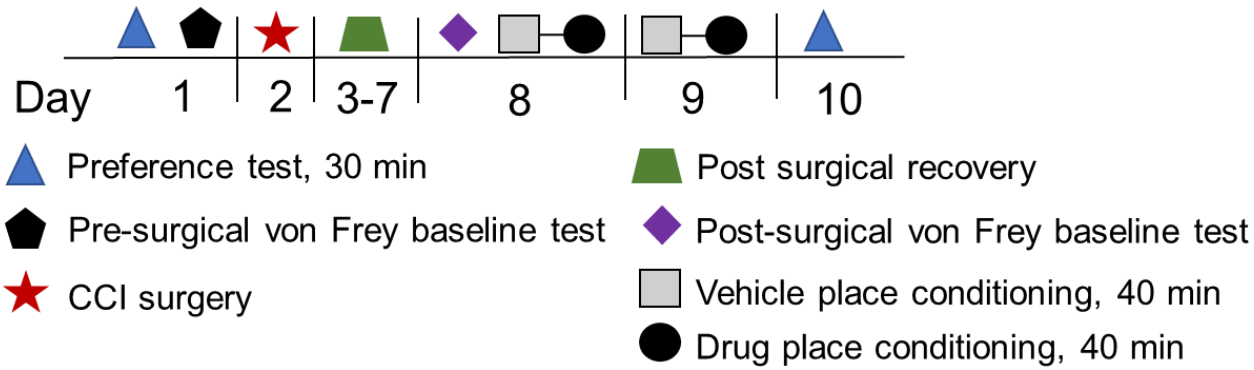

To assess the antinociceptive effect of compounds under an operant condition, mice were tested in a procedure modified from Hummel et al.[25] and Salte et al. [26] (see schematic above) as we described recently[20]. One day prior to CCI surgery, naïve C57BL/6J mice were subjected to initial place preference testing in a three-chambered conditioned place preference apparatus where they were allowed to roam freely for 30 min, as described above. These same mice then underwent chronic constrictive nerve injury and were confirmed after 7 days to demonstrate mechanical allodynia, as detailed above. Allodynic mice were then subjected to 2 days of counterbalanced place conditioning, and the final place preference was assessed, as described above. For place conditioning, mice were treated with vehicle (i.p.) and then randomly confined to one of the outer chambers of the CPP apparatus for 40 min. Four hours later, the mice were administered *(icv*)

U50,488 (100 nmol), or C6 guano (100, nmol) and then confined to the opposite outer compartment of the apparatus. The conditioning was repeated on a second day, and the next day mice were given free access to each compartment of the apparatus for 30 min to determine the final place preference. Data are plotted as the difference in time spent in the drug-paired versus vehicle-paired compartment.

Pharmacokinetic Study

C6 guano was administered to mice *icv* at 100 nmol dose in four C57BL/6J mice. At 20 min post administration of the drug, mice were anesthetized under isoflurane, blood was removed, and animals were sacrificed for brain removal. Brains were quickly rinsed off with PBS, blot-dried and snap frozen. Tissue samples were then weighed and placed into Navy bead lysis kit tubes. Naïve tissue was used to prepare Standard, Quality control (QC) and Blanks samples in tissue matrix. To each sample tube was added the appropriate volume of cold acetonitrile:water (3:1) to achieve a tissue concentration of 200 mg/mL. Tubes were placed in a bead beater for 3 minutes then centrifuged at 3200 rpm for 5 minutes at 4°C. The supernatants were transferred in Eppendorf tubes and stored at −80 °C until the day of analysis. The day of the analysis, The samples were thawed on ice, mixed vigorously then centrifuged at 3200 rpm for 5 minutes at 4°C. Supernatant (30 µl) were collected and transferred into a 96-well plate. In the same way, 30µl of Standards, QC, Blanks and Double blanks samples freshly made in the matrix were transferred into the plate. Then cold Acetonitrile (150 µl) spiked with internal standard (IS) was added to blanks, standards, QCs and unknown samples. Only cold acetonitrile (150 µl) was added to the double blanks. Samples were mixed vigorously for 10 min then centrifuged at 3200 rpm for 10 minutes at 4°C. Supernatant were transferred into a 96-well plate, evaporated to dryness under nitrogen at RT. Samples were reconstituted in 100 µL of 0.1% v/v formic acid in water:acetonitrile (90:10). Plate was sealed, vortexed during 5min, briefly centrifuged then submitted for LC/MS analysis as described previously.[23]

Brain homogenate stability

Freshly isolated mouse brain was gently homogenized in phosphate buffered saline (1:3, w:v). Homogenate was spiked with C6 guano at a final concentration of 10 µM and a DMSO concentration of 0.1%. Duplicate samples were incubated at 37C on an orbital shaker. Aliquots were removed at 0, 5, 15, 60, 120, 180, and 240 minutes and immediately quenched with 2-times v:v acetonitrile containing an internal standard. Samples were filtered and analyzed by LC-MS/MS and the peak area of analyte/IS was used to determine the amount of compound remaining. Time vs the natural log of % remaining was plotted and the slope was fit to -ln(2)/slope to calculate the half-life.

Instrument Settings

LC (Shimadzu UFLC XR) conditions

Compound	C6 guano	I.S. (Propranolol)
Column	Thermo Betasil C18 5µ, 50x2.1mm	
Mobile phase	A: Water with 0.1% Formic Acid B: Acetonitrile with 0.1% Formic Acid	
Flow rate (ml/min)	0.35	
Temperature (°C)	35	
Injection volume(µl)	5.0	
Retention Time (min)	0.35	1.9

Gradient elution conditions:

Time (min)	Mobile phase A (%)	Mobile phase B (%)
0.1	90	10

0.3	90	10
0.8	5	95
1.5	5	95
2.8	90	10
3.6	90	10

MS (API6500) conditions

Compound	C6 guano	I.S. (Propranolol)
MRM(+)	402.3/188.1	260.1/183.2
Collision Gas	7	
Curtain GAS	25	
Ion Source Gas1	25	
Ion Source Gas2	25	
Ion Spray Voltage	5500	
Temperature (°C)	550	
Collision Energy	20	70
Declustering Potential	40	25
Entrance Potential	10	

S2: Procedure and Synthetic Schemes for Fentanyls-Bitopics

Chemical Synthesis

Here we synthesized a small library of compounds, specifically fentanyl derivatives with a bitopic extension aiming at reaching the allosteric site and specifically the sodium binding pocket. In order to do so, we replaced the classical fentanyl benzene ring by an aliphatic chain linker grafted to a nitrogen-containing "warhead", amine or guanidine being our primary choice in this case. In recent years, a certain procedure was reported that we modified in order to efficiently obtain the desired molecules.

As such, we selectively protected the starting diamino material using the *tert*-butyloxycarbonyl group, the first step of this reaction consisting in selectively activating one amine by *in situ* monohydrochlorination with chlorotrimethylsilane. The following reductive amination was performed in the presence of an excess of sodium cyanoborohydride and AcOH, found to be efficient with primary amines and ketone/aldehyde reagents, which yielded compound **3** in moderate yield. The secondary amine was then *N*-acetylated in the presence of Hunig's base (DIPEA) to provide the corresponding tertiary amine **4**. Next, deprotection of the *tert*-butyloxycarbonyl group was performed using HCl 4M in dioxane, and yielded the fentanyl amino-bitopics in quantitative yields. Likewise, the next intermediate was prepared by reacting bis-Boc-thiourea in the presence of copper chloride and afforded the bis-Boc protected guanidine **6.** Finally, deprotection was carried out and afforded the desired final guano-fentanyl bitopics **7** in excellent yields.

Supplementary Figure 1

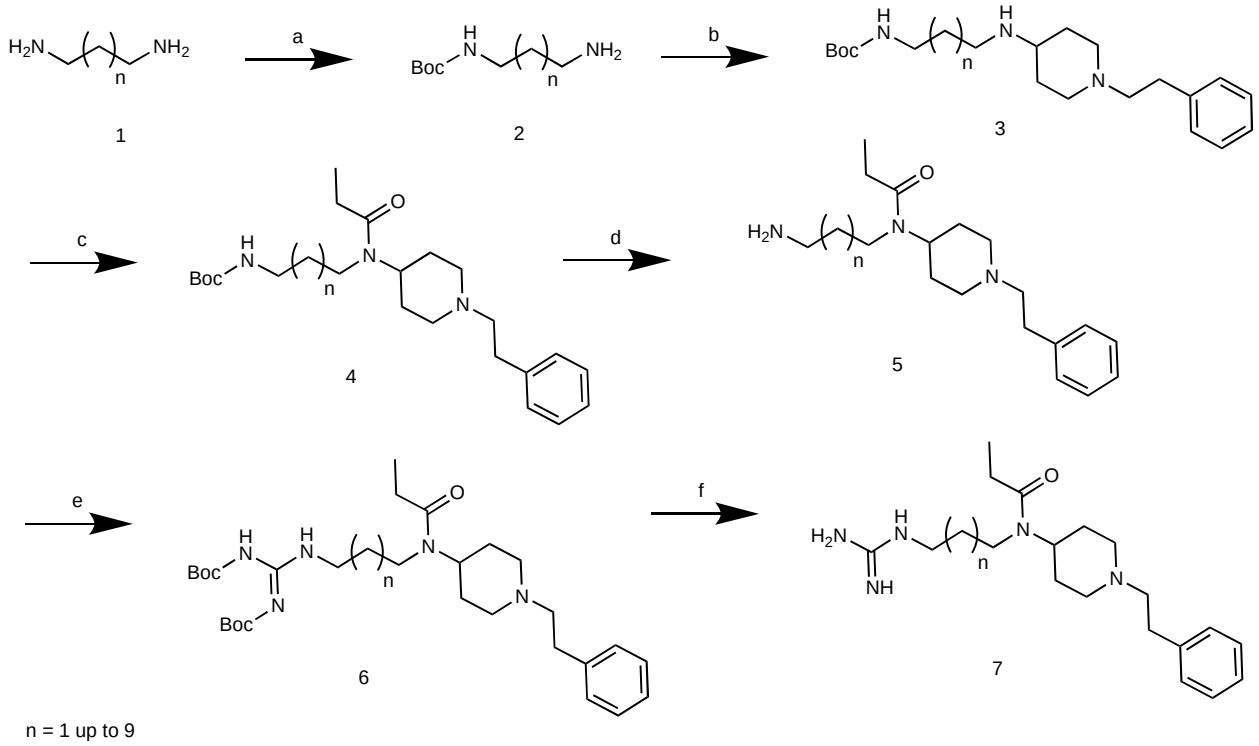

Synthesis of fentanyl bitopics. Reagents and conditions: (a) Me_3SiCl, H_2O, Boc_2O, MeOH, 89-91%. (b) 1-phenethylpiperidin-4-one, $NaBH_3CN$, AcOH, MeOH, MS 3Å, overnight, 47-62%. (c) PrCl, DIPEA, DCM, 39-45%. (d) HCl / Dioxane, rt, 16h, 81-92%. (e) bis-Boc thiourea, CuCl, 52-65%. (I), THF; (f) HCl / Dioxane, rt, 16h, 81-92%.

Fentanyl-bitopics (See **Supplementary Figure 1**)

Step a, Boc protection: To the corresponding diamine (1 g, 10 mmol) was added anhydrous methanol at 0ºC under stirring, followed by the dropwise addition of freshly distilled Me_3SiCl (1.08 g, 10 mmol). A white precipitate appeared at the bottom of the flask, the mixture was allowed to come to RT and water (1 mL) followed by Boc_2O (2.18 g, 10 mmol) in MeOH (3 mL) was added. The mixture was stirred at RT for 1h, diluted with water (50 mL) and the aqueous layer washed with ether (2 × 75 mL). The aqueous layer was adjusted to pH >12 with 2N NaOH and extracted into dichloromethane (3 × 50 mL). The combined organic layers were dried over anhydrous Na_2SO_2 and solvent removal gave the corresponding as a light yellow oil, which was

used in the next step without further purification (1.56 g, 78% for **C5 guano**, 78-91% for others selected bitopics).

Step b, reductive amination: $NaBH_3CN$ (100 mg, 1.6 mmol) was added to a 0.2 M solution of 1-phenethyl-4-piperidone (203 mg, 1 mmol), mono-Boc-protected diamine (243 mg, 1.2 mmol) and 3A molecular sieves in 5mL dry MeOH. The pH of the reaction was adjusted to 6–7 with AcOH during the course of the reaction. The reaction was stirred for 5h, and then filtered on a pad of Celite. The filtrate was concentrated under vacuum and the crude product was purified by flash column chromatography (EtOAc/hexanes) to afford the secondary corresponding amine as a light yellow oil (238 mg, 51% for **C5 guano**, 47-62% for others selected bitopics).

Step c, acylation: The secondary amine starting material (235 mg, 0.6 mmol) was dissolved in methylene chloride (5 mL) in a 25 mL round bottom flask equipped with a small stir bar and was treated with diisopropylethylamine (0.16 mL, 116 mg, 0.6 mmol). The solution was cooled with an ice bath and treated dropwise with propionyl chloride (53 µL, 55 mg, 0.6 mmol). The resulting mixture was stirred for 2h at ambient temperature. The mixture was transferred to a separatory funnel and partitioned (CH_2Cl_2/H_2O). The organic phase was washed with brine, saturated $NaHCO_3$, dried over anhydrous Na_2SO_4 and evaporated *in vacuo* at 40ºC to give a yellow oil that was purified by flash column chromatography (3:7 to 7:3 EtOAc/hexanes) to afford the tertiary corresponding amine as a light yellow oil (234 mg, 88% for **C5 guano**, 39-88% for others selected bitopics).

Step d, Boc deprotection: Boc-amine (234 mg, 0.5 mmol) was dissolved in dry MeOH (1 mL) and 4M HCl in dioxane (2.5 mL) was added. The mixture was allowed to stir at room temperature overnight. The reaction mixture was concentrated *in vacuo*, washed and triturated with ether, then

concentrated to give the deprotected amine as a white powder (155 mg, 90% for **C5 guano**, 81-92% for other selected bitopics).

Step e, Synthesis of Boc protected guanylated derivatives: To a mixture of amine salt (103 mg, 0.3 mmol), bis-Boc-thiourea (80 mg, 0.3 mmol) and Et_3N (100 mg, 1 mmol) in dimethylformamide (1 mL) at 0ºC was added cooper chloride (45 mg, 1.1 mmol) with stirring. The resulting mixture was stirred at 0ºC for 1h, diluted with ethyl acetate (20 mL), and filtered through a pad of celite. The filtrate solution was washed with water and brine, dried over Na_2SO_4 and concentrated *in vacuo*. The residue was purified by flash column chromatography (3:7 to 7:3 EtOAc/hexanes) to afford the protected guanidine derivative as a yellow solid (99 mg, 59% for **C5 guano**, 52-65% for other selected bitopics).

Step f, Boc-deprotection: The guanidine protected (99 mg, 0.18 mmol) was dissolved in dry MeOH (0.35 mL) and 4M HCl in dioxane (1 mL) was added. The mixture was allowed to stir at room temperature overnight. The reaction mixture was concentrated *in vacuo*, washed and triturated with ether, then concentrated to give the deprotected guanidine as a white powder (74 mg, 89% for **C5 Guano**, 89-91% for other selected bitopics).

S3: Spectral data of Fentanyls-Bitopics

C3 amino
N-(3-aminopropyl)-*N*-(1-phenethylpiperidin-4-yl)propionamide
Chemical Formula: $C_{19}H_{31}N_3O$
^{1}H NMR (400 MHz, Methanol-d_4) δ 7.74 – 7.41 (m, 5H), 4.63 – 4.33 (m, 1H), 4.11 – 3.81 (m, 3H), 3.79 – 3.62 (m, 3H), 3.53 – 3.12 (m, 6H), 2.90 – 2.39 (m, 4H), 2.37 – 2.02 (m, 4H), 1.52 – 1.33 (m, 4H).

C3 guano
N-(3-guanidinopropyl)-*N*-(1-phenethylpiperidin-4-yl)propionamide
Chemical Formula: $C_{20}H_{33}N_5O$
^{1}H NMR (400 MHz, Methanol-d_4) δ 7.56 (dt, *J* = 20.3, 5.0 Hz, 5H), 4.49 (d, *J* = 47.8 Hz, 1H), 4.11 – 3.82 (m, 3H), 3.61 (s, 2H), 3.54 – 3.30 (m, 6H), 2.85 – 2.49 (m, 4H), 2.35 – 1.96 (m, 4H), 1.49 – 1.31 (m, 3H).

C5 amino
N-(5-aminopentyl)-*N*-(1-phenethylpiperidin-4-yl)propionamide
Chemical Formula: $C_{21}H_{35}N_3O$
^{1}H NMR (400 MHz, Methanol-d_4) δ 7.40 – 7.17 (m, 5H), 4.35 – 4.05 (m, 1H), 3.71 (s, 2H), 3.16 (dq, *J* = 43.1, 8.7 Hz, 5H), 2.93 (d, *J* = 8.1 Hz, 2H), 2.38 (ddt, *J* = 42.1, 26.2, 10.5 Hz, 4H), 2.05 – 1.84 (m, 2H), 1.80 – 1.18 (m, 7H), 1.10 (dd, *J* = 9.1, 5.6 Hz, 3H).
^{13}C NMR (101 MHz, Methanol-d_4) δ 176.63, 176.08, 137.64, 130.00, 129.82, 128.31, 59.04, 53.65, 53.24, 52.59, 46.42, 40.57, 31.48, 31.23, 29.79, 28.85, 28.18, 27.96, 27.85, 27.66, 24.73, 9.99.
HRMS calcd for $C_{22}H_{37}N_5O$ (MH+), 346.285289; found, 346.285597.

C5 guano
N-(5-guanidinopentyl)-*N*-(1-phenethylpiperidin-4-yl)propionamide
Chemical Formula: $C_{22}H_{37}N_5O$
^{1}H NMR (400 MHz, Methanol-d_4) δ 7.43 – 7.21 (m, 5H), 4.21 (d, *J* = 51.3 Hz, 1H), 3.73 (s, 3H), 3.53 (d, *J* = 42.8 Hz, 1H), 3.29 – 2.81 (m, 8H), 2.61 – 2.16 (m, 4H), 1.97 (t, *J* = 19.1 Hz, 2H), 1.80 – 1.52 (m, 4H), 1.43 (s, 2H), 1.13 (q, *J* = 7.1 Hz, 3H).
^{13}C NMR (101 MHz, Methanol-d_4) δ 176.63, 176.06, 158.64, 137.66, 129.99, 128.29, 59.09, 53.69, 53.29, 52.50, 46.49, 42.34, 31.49, 29.93, 29.47, 29.30, 28.93, 27.92, 27.72, 25.16, 25.00, 10.02.
HRMS calcd for $C_{22}H_{37}N_5O$ (MH+), 388.307087; found, 388.307324.

C6 amino
N-(6-aminohexyl)-*N*-(1-phenethylpiperidin-4-yl)propionamide
Chemical Formula: $C_{22}H_{37}N_3O$
^{1}H NMR (400 MHz, Methanol-d_4) δ 7.41 – 7.18 (m, 5H), 4.36 – 4.04 (m, 1H), 3.70 (d, *J* = 10.9 Hz, 2H), 3.28 – 3.02 (m, 7H), 2.94 (d, *J* = 8.6 Hz, 2H), 2.55 – 2.20 (m, 4H), 2.06 – 1.85 (m, 2H), 1.75 – 1.24 (m, 9H), 1.10 (td, *J* = 7.2, 2.6 Hz, 3H).

C6 guano
N-(6-guanidinohexyl)-*N*-(1-phenethylpiperidin-4-yl)propionamide
Chemical Formula: $C_{23}H_{39}N_5O$
^{1}H NMR (400 MHz, Methanol-d_4) δ 7.45 – 7.20 (m, 5H), 4.21 (d, *J* = 51.5 Hz, 1H), 3.73 (s, 3H), 3.53 (d, *J* = 40.8 Hz, 1H), 3.34 (s, 2H), 3.27 – 3.04 (m, 7H), 2.64 – 2.19 (m, 4H), 1.97 (t, *J* = 19.0 Hz, 2H), 1.80 – 1.52 (m, 4H), 1.43 (s, 2H), 1.24 – 1.00 (m, 3H).

C7 amino
N-(7-aminoheptyl)-*N*-(1-phenethylpiperidin-4-yl)propionamide
Chemical Formula: $C_{23}H_{39}N_3O$
^{1}H NMR (400 MHz, Methanol-d_4) δ 7.22 (dq, *J* = 13.1, 7.3, 6.7 Hz, 5H), 4.15 – 3.93 (m, 1H), 3.62 (d, *J* = 11.4 Hz, 2H), 3.05 (d, *J* = 49.0 Hz, 5H), 2.83 (t, *J* = 7.6 Hz, 2H), 2.46 – 2.19 (m, 3H), 2.16 – 1.77 (m, 3H), 1.50 (d, *J* = 42.0 Hz, 4H), 1.32 (s, 7H), 1.02 (t, *J* = 6.4 Hz, 3H).

C7 guano
N-(7-guanidinoheptyl)-*N*-(1-phenethylpiperidin-4-yl)propionamide
Chemical Formula: $C_{24}H_{41}N_5O$
^{1}H NMR (400 MHz, Methanol-d_4) δ 7.28 (tt, *J* = 13.7, 7.3 Hz, 5H), 4.15 (d, *J* = 52.1 Hz, 1H), 3.70 (d, *J* = 11.7 Hz, 2H), 3.21 – 2.90 (m, 7H), 2.56 – 2.06 (m, 4H), 2.06 – 1.84 (m, 2H), 1.54 (d, *J* = 29.8 Hz, 5H), 1.37 (s, 7H), 1.10 (td, *J* = 7.4, 3.6 Hz, 4H).

C9 amino
N (9-aminononyl)-*N*-(1-phenethylpiperidin-4-yl)propionamide
Chemical Formula: $C_{25}H_{43}N_3O$
^{1}H NMR (400 MHz, Methanol-d_4) δ 7.43 – 7.21 (m, 5H), 4.15 (d, *J* = 13.9 Hz, 1H), 3.71 (d, *J* = 12.1 Hz, 2H), 3.40 – 3.34 (m, 6H), 3.26 – 3.03 (m, 5H), 2.56 – 2.32 (m, 3H), 2.18 (d, *J* = 10.4 Hz, 1H), 1.98 (dd, *J* = 26.3, 13.6 Hz, 2H), 1.73 – 1.49 (m, 4H), 1.39 (s, 11H).

C9 guano
N (9-guanidinononyl)-*N*-(1-phenethylpiperidin-4-yl)propionamide
Chemical Formula: $C_{26}H_{45}N_5O$
^{1}H NMR (400 MHz, Methanol-d_4) δ 7.28 (q, *J* = 15.0, 11.4 Hz, 5H), 4.18 (d, *J* = 49.8 Hz, 1H), 3.70 (s, 2H), 3.46 (q, *J* = 7.1 Hz, 1H), 3.33 (s, 2H), 3.14 (dd, *J* = 14.0, 6.8 Hz, 6H), 2.67 – 2.17 (m, 4H), 1.94 (t, *J* = 19.8 Hz, 2H), 1.57 (s, 4H), 1.34 (d, *J* = 9.3 Hz, 10H), 1.12 (dt, *J* = 22.6, 7.4 Hz, 5H).

C11 amino
N (11-aminoundecyl)-*N*-(1-phenethylpiperidin-4-yl)propionamide
Chemical Formula: $C_{27}H_{47}N_3O$
^{1}H NMR (400 MHz, Methanol-d_4) δ 7.37 – 7.19 (m, 5H), 4.14 (d, *J* = 12.0 Hz, 1H), 3.79 – 3.61 (m, 5H), 3.37 – 3.31 (m, 4H), 3.23 – 3.02 (m, 5H), 2.49 – 2.29 (m, 3H), 2.27 – 2.10 (m, 1H), 1.96 (dd, *J* = 28.3, 13.6 Hz, 2H), 1.62 (d, *J* = 9.5 Hz, 4H), 1.34 (d, *J* = 10.4 Hz, 16H).

^{13}C NMR (101 MHz, Methanol-d_4) δ 175.19, 128.59, 128.35, 126.91, 66.70, 65.46, 57.63, 52.26, 51.64, 39.34, 30.03, 29.34, 29.20, 29.10, 29.03, 28.84, 27.59, 27.18, 26.60, 26.47, 26.05, 13.99.
HRMS calcd for $C_{27}H_{47}N_3O$ (MH+) 430.379190; found, 430.379205.

C11 guano
N-(11-guanidinoundecyl)-N-(1-phenethylpiperidin-4-yl)propionamide
Chemical Formula: $C_{28}H_{49}N_5O$
^{1}H NMR (400 MHz, Methanol-d_4) δ 7.36 – 7.04 (m, 5H), 4.10 (d, J = 45.2 Hz, 1H), 3.69 – 3.41 (m, 4H), 3.10 – 2.96 (m, 5H), 2.44 – 2.06 (m, 4H), 1.87 (dd, J = 26.1, 13.6 Hz, 2H), 1.61 – 1.36 (m, 5H), 1.25 (q, J = 5.4 Hz, 16H), 1.09 – 0.96 (m, 3H).
^{13}C NMR (101 MHz, Methanol-d_4) δ 176.64, 137.61, 129.99, 129.83, 128.30, 68.14, 59.07, 53.67, 53.26, 52.71, 46.92, 42.50, 31.94, 31.47, 30.75, 30.62, 30.43, 30.34, 30.26, 29.89, 28.98, 28.03, 27.92, 27.71, 10.01.
HRMS calcd for $C_{28}H_{49}N_3O$ (MH+) 472.400988; found, 472.400576.

S4: Additional Extended Data Tables and Figures

Supplementary Figure 2: Potency heatmap

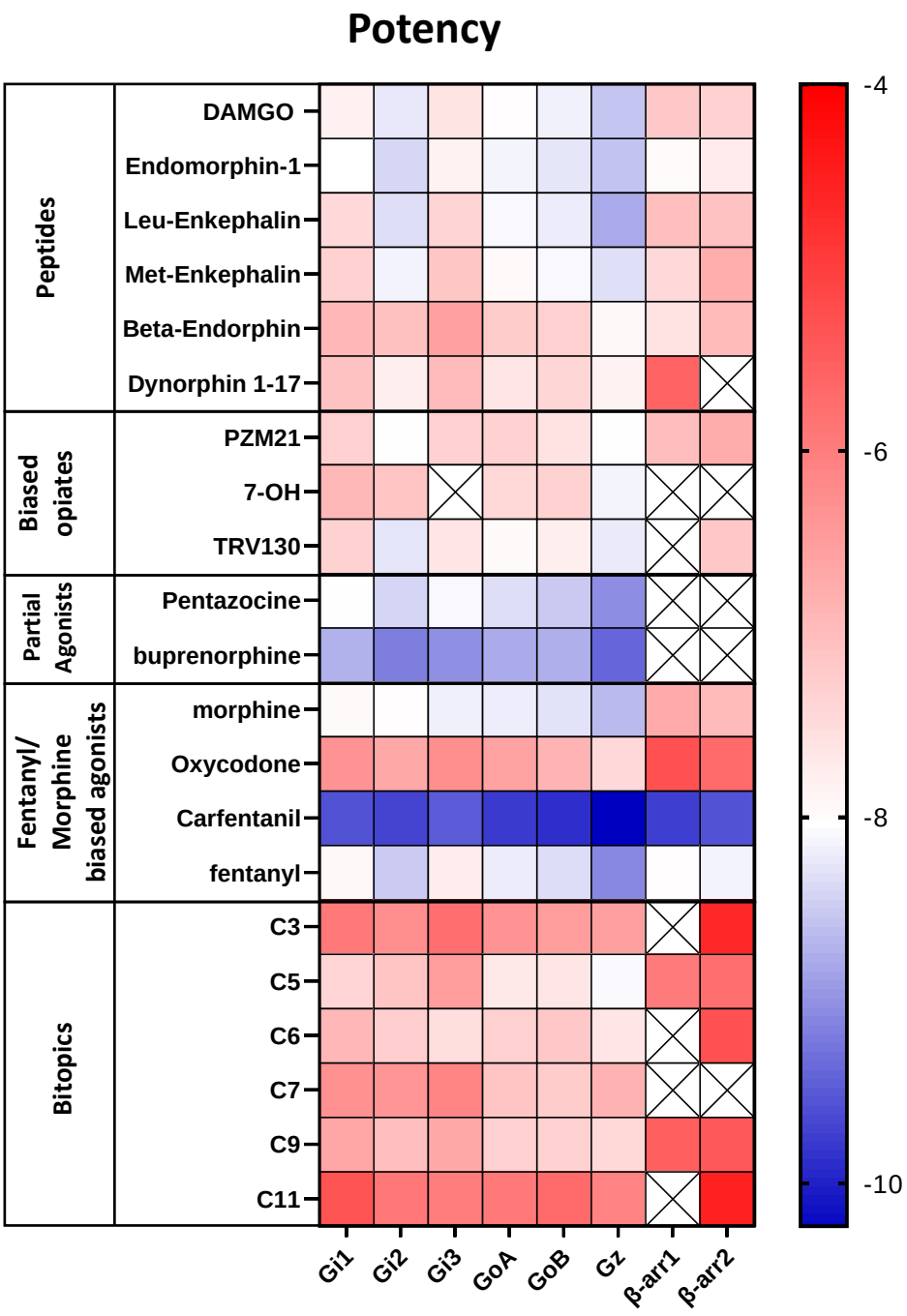

Heatmap represents potencies of opioid peptides, biased agonists, partial agonists, morphine/fentanyl template agonists and bitopics using TRUPATH and arrestin1/2 activity.

Supplementary Table 1: Characterization of lead bitopics and other μOR controls at mμOR and off target activity of lead bitopics.

A)

Ligands	Binding	
	Ki nM (pK_i ± SEM)	
	hMOR	mMOR
DAMGO	2.4 (8.7 ± 0.05)	2.2 (8.7 ± 0.05)
C5 guano	1.05 (9.0 ± 0.05)	0.62 (9.2 ± 0.06)
C6 guano	1.2 (8.9 ± 0.1)	1.08 (9.0 ± 0.08)
Fentanyl	0.88 (9.1 ± 0.05)	0.67 (9.2 ± 0.05)
Morphine	0.43 (9.4 ± 0.04)	0.41 (9.4 ± 0.04)
7OH	7.9 (8.1 ± 0.1)	7.69 (8.1 ± 0.1)

B)

Ligands	Gi1			β-arrestin2		
	EC_{50} (nM)	pEC_{50} ± SEM	E_{max} ± SEM (%)	EC_{50} (nM)	pEC_{50} ± SEM	E_{max} ± SEM (%)
DAMGO	6.6	8.2 ± 0.04	100.0 ± 1.2	32.9	7.5 ± 0.8	100.0 ± 2.7
C5 guano	25.0	7.6 ± 0.05	94.7 ± 1.6	3,457	5.5 ± 0.3	23.3 ± 3.5
C6 guano	39.0	7.4 ± 0.06	79.3 ± 1.8	12,910	4.9 ± 0.3	25.7 ± 4.7
Fentanyl	5.5	8.3 ± 0.05	100.5 ± 2.0	39.7	7.4 ± 0.06	95.5 ± 1.8
Morphine	100.5	7.0 ± 0.06	98.9 ± 2.7	12,410	4.9 ± 0.2	32.0 ± 5.0
7OH	122.9	6.9 ± 0.07	56.3 ± 1.7	n.d.	n.d.	<20

C)

Receptor	C5-guano		C6-guano	
	K_i (nM)	SEM	K_i (nM)	SEM
μOR	**6.1**	**0.91**	**2.7**	**0.21**
κOR	**225**	**36**	**259**	**31**
δOR	**1530**	**176**	**312**	**62**
H1	**274**	**87**	**1107**	**235**
Alpha2A	**4816**	**313**	**-**	**-**
Alpha1A	**-**	**-**	**910**	**202**

A) K_i binding competition studies were performed with the indicated compound against ^{3}DAMGO (1 nM) in membranes from HEK293T cells transiently expressing the human or mouse MOR. Results are presented as pK_i ± SEM from three independent experiments performed in triplicate.

B) Pharmacological parameters of mouse MOR for Gi1 and β-arrestin2. Potency [EC_{50} nM (pEC_{50} ± SEM)] and efficacy [E_{max} ± SEM (%)] are reported as estimates from simultaneous curve fitting of all biological replicates and include standard error.

C) Binding affinities reported were conducted by the National Institute of Mental Health Psychoactive Drug Screening Program (NIMH-PDSP). Details of the methods and radioligands used for the binding assays are available on the NIMH-PDSP website at https://pdspdb.unc.edu/pdspWeb/content/PDSP%20Protocols%20II%202013-03-28.pdf.

Supplementary Figure 3. Gi-1 signaling of lead bitopics at κOR and δOR. A/ C6 guano did not signal through δOR while C5 guano had poor potency. B/C6 guano has low efficacy at κOR. C/ Efficacy and potency values for lead bitopics. DPDPE and U50,488H were used as appropriate controls for δOR and κOR.

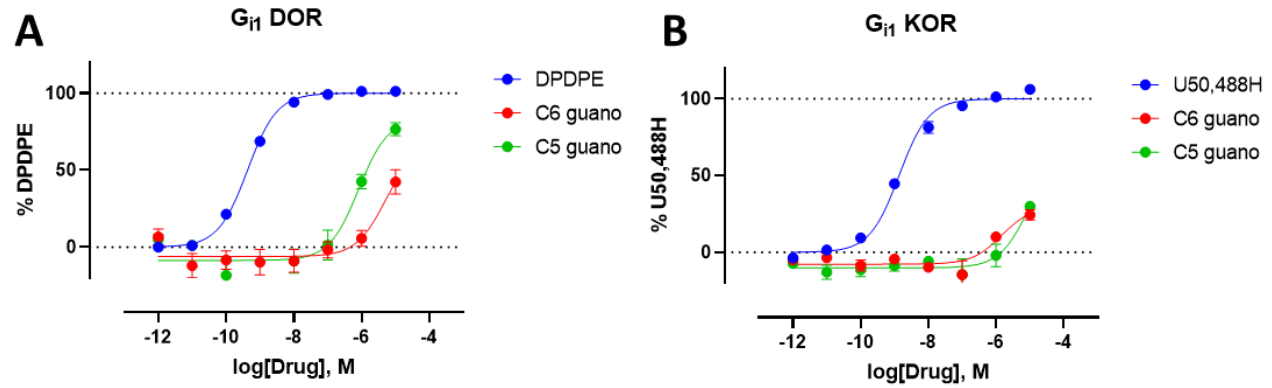

C

Ligands	G_{i1} DOR		G_{i1} KOR	
	EC_{50} nM (pEC_{50} ± SEM)	Efficacy (Emax % ± SEM)	EC_{50} nM (pEC_{50} ± SEM)	Efficacy (Emax % ± SEM)
DPDPE/ U50,488H	0.43 (9.4 ± 0.1)	100 ± 1.1	1.4 (8.9 ± 0.1)	100 ± 3.1
C6-guano	n.d.	n.d.	1460 (5.8 ± 0.3)	38 ± 6.9
C5-guano	811 (6.1 ± 0.2)	92 ± 12.0	n.d.	n.d.

Supplementary Figure 4. Characterization of morphine antinociception, metabolic stability and brain exposure of C6 guano and respiratory depression of morphine.

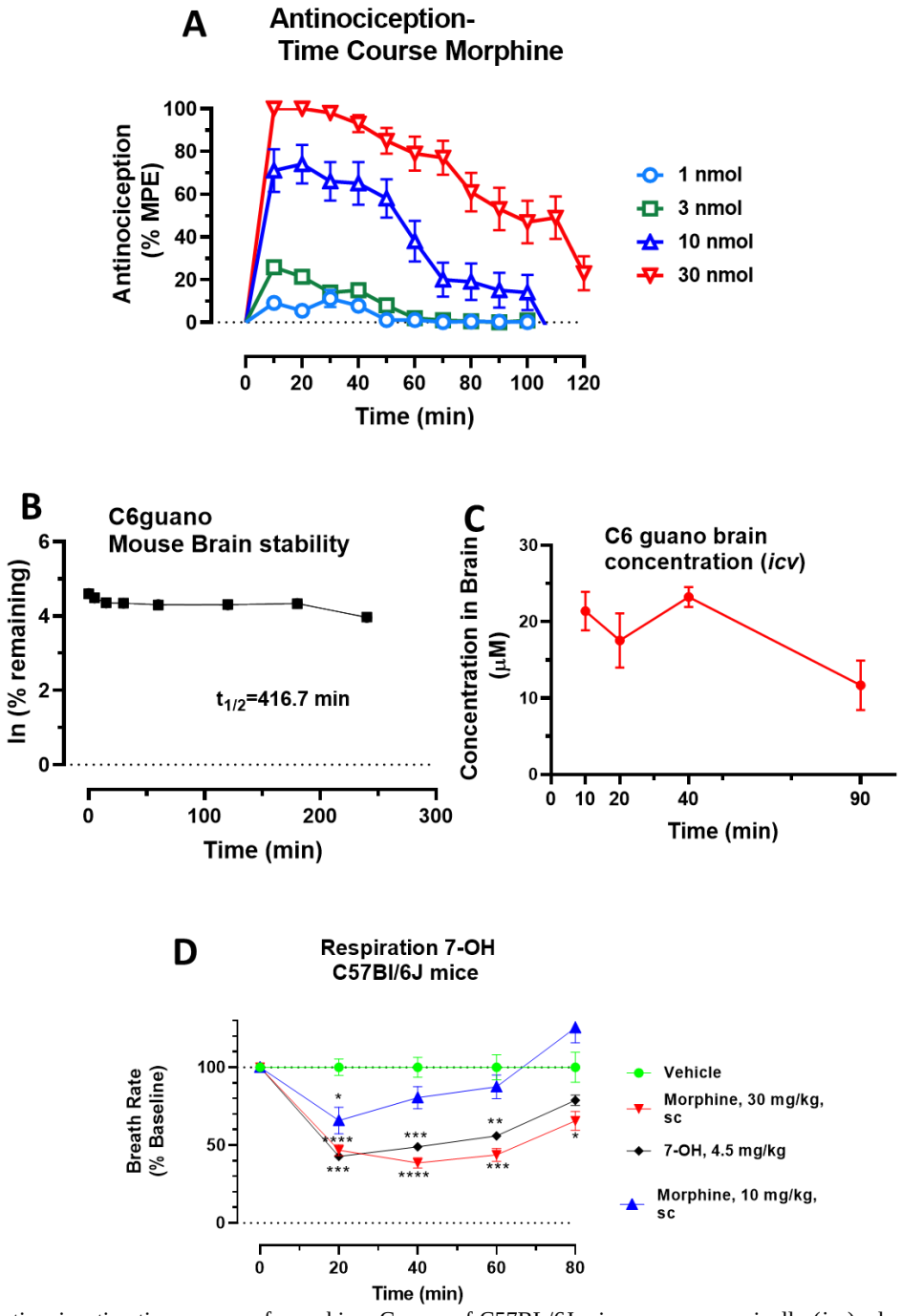

A) Antinociceptive time course of morphine: Groups of C57BL/6J mice were supraspinally (*icv*) administered morphine at doses of 1, 3, 10 and 30 (n = 8 each group) with repeated measures over time and antinociception measured using the 55°C tail withdrawal assay.

B) Stability of lead bitopic in mouse brain homogenate. C6 guano was incubated with mouse brain homogenate and metabolic stability followed using LC-MS/MS for 4h.

C) Brain exposure of C6 guano. C6 guano was administered *icv* in 4 C57BL6J mice per time point and concentration of drug determined using LC-MS/MS.

D) Respiratory depression of biased agonist 7OH in C57BL6J mice. Mice were administered either vehicle (n = 12), morphine (10 and 30 mg/kg, sc; n = 12), or 7OH (4.5 mg/kg, sc; n = 12), and the breath rates was measured every 20 min for 180 min. Morphine administered sc caused reduction in the breath rate with respect to saline at 20 min (*p=0.03) at 10 mg/kg, sc dose. Greater decrease in breath rates were seen at 15x antinociceptive ED_{50} dose of 30 mg/kg, sc (**p = 0.0021), 40 min (***p = 0.0003) and 60 min (**p = 0.0010) post drug administration. 7OH similarly respiratory depression similar to morphine at 20 min (****p<0.0001), 40 min (***p=0.0006) and 60 min (**p=0.0034) as determined by 2-way ANOVA followed by Dunnett's multiple-comparison test.

Supplementary Table 2: Statistical analysis of Figure 3a-b and Figure 4a-i.

Figure	Panel title/Variable	Statistical Model	Test statistic	p-value	Number per group
3a	β-arrestin2 recruitment of bitopics Treatment	One-way ANOVA followed Tukey's multiple comparisons test	F(5,36)=26.70)	****p<0.0001	3-6
	C5guano vs. DAMGO	One-way ANOVA followed Tukey's multiple comparisons test		****p<0.0001	3 (C5) 6(DAMGO)
	C5guano vs. Fentanyl	One-way ANOVA followed Tukey's multiple comparisons test		***p=0.0003	3
	C6guano vs. DAMGO	One-way ANOVA followed Tukey's multiple comparisons test		****p<0.0001	3 (C6) 6(DAMGO)
	C6guano vs. Fentanyl	One-way ANOVA followed Tukey's multiple comparisons test		****p<0.0001	3
	7-OH vs. DAMGO	One-way ANOVA followed Tukey's multiple comparisons test		****p<0.0001	3 (7OH) 6(DAMGO)
3b	β-arrestin1 recruitment of bitopics Treatment	One-way ANOVA followed Tukey's multiple comparisons test	F (6, 38) = 99.16	****p<0.0001	3-6
	C5guano vs. DAMGO	One-way ANOVA followed Tukey's multiple comparisons test		****p<0.0001	3 (C5) 6(DAMGO)
	C5guano vs. Fentanyl	One-way ANOVA followed Tukey's multiple comparisons test		****p<0.0001	3
	C6guano vs. DAMGO	One-way ANOVA followed Tukey's multiple comparisons test		****p<0.0001	3 (C6) 6(DAMGO)
	C6guano vs. Fentanyl	One-way ANOVA followed Tukey's multiple comparisons test		****p<0.0001	3
	7-OH vs. DAMGO	One-way ANOVA followed Tukey's multiple comparisons test		****p<0.0001	3 (7OH) 6(DAMGO)
4a	Thermal Antinociception				8

4b	Thermal Antinociception Row factor		F (5, 205) = 4.036	**p=0.0016	8-12
	C6-guano WT vs. Vehicle	Two-way ANOVA followed by Dunnett's multiple comparison test		10-30 min ****p<0.0001 40min***p=0.0003	C6 WT (12) Vehicle (11)
	C6-guano WT vs. C6-guano µOR KO	Two-way ANOVA followed by Dunnett's multiple comparison test		10-20 min ****p<0.0001 30 min *p=0.0041	C6 WT (12) µOR KO (10)
	vehicle µOR vs C6-guano µOR	Unpaired two tailed t-tests with Welsch's correction			8
4c	Locomotor effect Row factor	Two-way ANOVA followed by Dunnett's posthoc	F (8, 869) = 7.638	****p<0.0001	12-24
	Morphine 10 nmol vs. saline icv	Two-way ANOVA followed by Dunnett's posthoc		160 min ***p=0.0001	Morphine (12) Saline (12)
	Morphine 30 nmol vs. saline icv	Two-way ANOVA followed by Dunnett's posthoc		120 min **p=0.0075 140 min *p=0.0457 160 min ****p<0.0001	Morphine (18) Saline (12)
	Morphine 100 nmol vs. saline icv	Two-way ANOVA followed by Dunnett's posthoc		120 min **p=0.0013 140 min **p=0.0006 160 min ****p<0.0001	Morphine (16) Saline (12)
	C6guano 300 nmol vs. vehicle icv	Unpaired two tailed t-tests with Welsch's correction		ns	C6 (12) vehicle (24)
4d	Respiratory Depression Morphine group Time x column factor	Two-way ANOVA followed by Dunnett's multiple comparison test	F (12, 276) = 2.150	*p=0.0143	12-18
	Morphine 10 nmol vs. saline icv	Two-way ANOVA followed by Dunnett's multiple comparison test		ns	Morphine (16) Saline (12)
	Morphine 30 nmol vs. saline icv	Two-way ANOVA followed by Dunnett's multiple comparison test		20 min *p=0.016 40 min *p=0.02	Morphine (18) Saline (12)

	Morphine 100 nmol vs. saline icv	Two-way ANOVA followed by Dunnett's multiple comparison test		20 min ***p=0.0004 40 min **p=0.0086	Morphine (16) Saline (12)
	Respiratory Depression C6 guano group Time x column factor	Two-way ANOVA followed by Dunnett's multiple comparison test	F (16, 344) = 7.006	****p<0.0001	12-24
	C6guano 100 nmol vs. vehicle icv	Two-way ANOVA followed by Dunnett's multiple comparison test		60 min **p=0.0012 80 min ***p=0.0004 100 min ***p=0.0003 120-140 ****p<0.0001 160 min **p=0.0011	C6 (12) Vehicle (24)
	C6guano 300 nmol vs. vehicle icv	Two-way ANOVA followed by Dunnett's multiple comparison test		40 min **p=0.0012 60-160 min ****p<0.0001 180 min *p=0.0399	C6 (12) Vehicle (24)
	C6guano 300 nmol WT vs. C6 guano µOR KO icv	Unpaired two tailed t-tests with Welsch's correction		ns	C6 (12) µOR KO (12)
4e	Conditioned place preference or aversion CPP / CPA				12-24
	CPP pre morphine vs post morphine	Unpaired two tailed t-tests with Welsch's correction	t=2.304, df=20.55	*p=0.03	12
	CPP pre-Saline vs post saline	Unpaired two tailed t-tests with Welsch's correction	t=0.9406, df=39.79	p=0.3526	21
	CPP pre C6guano vs post C6guano	Unpaired two tailed t-tests with Welsch's correction	t=0.06178, df=26.57	p=0.9512	22
	CPP pre U50,488H vs post U50,488H	Unpaired two tailed t-tests with Welsch's correction	t=2.728, df=29.24	*p=0.0107	24
	CPP pre-Vehicle vs post vehicle	Unpaired two tailed t-tests with Welsch's correction	t=1.188, df=38.38	p=0.2421	22
4f	Operant model of antinociception using constrictive nerve injury (CCI)-conditioned place preference (CPP)				17-23
	C6guano pre CPP vs post CPP	Unpaired two tailed t-tests with Welsch's correction	t=2.897, df=39.48	**p=0.0061	23

	U50,488H pre CPP vs post CPP	Unpaired two tailed t-tests with Welsch's correction	t=0.05483, df=25.35	p=0.9567	17
4g	Antinociception CCI model	Two-way ANOVA followed by Dunnett's multiple comparison test	F (3, 95) = 33.20	****p<0.0001	4-7
	C6guano 30 nmol vs vehicle	Two-way ANOVA followed by Dunnett's multiple comparison test		20 min ***p=0.0002 40 min **p=0.0063 60 min *p=0.0264 80 min *p=0.0393	Vehicle (4) C6(6)
	C6guano 100 nmol vs vehicle	Two-way ANOVA followed by Dunnett's multiple comparison test		20 min ***p=0.0004 40 min **p=0.0004 60 min *p=0.0038 80 min *p=0.0179 100 min *p=0.0106	Vehicle (4) C6 (6)
	C6 guano 10 nmol vs vehicle	Two-way ANOVA followed by Dunnett's multiple comparison test		ns	Vehicle (4) C6 (7)
4h	Antinociception writhing test	One-way ANOVA	F (2, 23) = 5.934	**p=0.0084	8-10
	C6guano vs. vehicle	One-way ANOVA		**p = 0.0075	Vehicle (10) C6(8)
	Morphine vs. vehicle	One-way ANOVA		*p = 0.0338	Vehicle (10) Morphine (8)
4i	Antinociceptive formalin				7-10
	C6guano vs. vehicle	Unpaired two tailed t-test with Welch's correction	t=4.793, df=15.84	***p =0.0002	Vehicle (10) C6(10)
	Morphine vs. Saline	Unpaired two tailed t-test with Welch's correction	t=2.639, df=11.84	*p = 0.0218	Saline (7) Morphine (9)

S5: Ethics declarations

Competing interests

S.M. and Y.X.P are scientific founders of a company, Sparian biosciences. B.K. is a founder of and consultant for ConfometRx, Inc. All other authors declare no competing interests.

S6: References

(1) Pickett, J. E.; Váradi, A.; Palmer, T. C.; Grinnell, S. G.; Schrock, J. M.; Pasternak, G. W.; Karimov, R. R.; Majumdar, S. Mild, Pd-Catalyzed Stannylation of Radioiodination Targets. *Bioorganic Med. Chem. Lett.* **2015**, *25* (8), 1761–1764.

(2) Majumdar, S.; Burgman, M.; Haselton, N.; Grinnell, S.; Ocampo, J.; Pasternak, A. R.; Pasternak, G. W. Generation of Novel Radiolabeled Opiates through Site-Selective Iodination. *Bioorganic Med. Chem. Lett.* **2011**, *21* (13), 4001–4004.

(3) Chakraborty, S.; Uprety, R.; Daibani, A. E.; Rouzic, V. L.; Hunkele, A.; Appourchaux, K.; Eans, S. O.; Nuthikattu, N.; Jilakara, R.; Thammavong, L.; Pasternak, G. W.; Pan, Y.-X.; McLaughlin, J. P.; Che, T.; Majumdar, S. Kratom Alkaloids as Probes for Opioid Receptor Function: Pharmacological Characterization of Minor Indole and Oxindole Alkaloids from Kratom. *ACS Chem. Neurosci.* **2021**, *12* (14), 2661–2678.

(4) Olsen, R. H. J.; DiBerto, J. F.; English, J. G.; Glaudin, A. M.; Krumm, B. E.; Slocum, S. T.; Che, T.; Gavin, A. C.; McCorvy, J. D.; Roth, B. L.; Strachan, R. T. TRUPATH, an Open-Source Biosensor Platform for Interrogating the GPCR Transducerome. *Nat. Chem. Biol.* **2020**, *16* (8), 841–849.

(5) Chakraborty, S.; DiBerto, J. F.; Faouzi, A.; Bernhard, S. M.; Gutridge, A. M.; Ramsey, S.; Zhou, Y.; Provasi, D.; Nuthikattu, N.; Jilakara, R.; Nelson, M. N. F.; Asher, W. B.; Eans, S. O.; Wilson, L. L.; Chintala, S. M.; Filizola, M.; Rijn, R. M. van; … Majumdar, S. A Novel Mitragynine Analog with Low-Efficacy Mu Opioid Receptor Agonism Displays Antinociception with Attenuated Adverse Effects. *J. Med. Chem.* **2021**, *64* (18), 13873–13892.

(6) DiBerto, J. F.; Olsen, R. H. J.; Roth, B. L. TRUPATH: An Open-Source Biosensor Platform for Interrogating the GPCR Transducerome. **2022**, *2525*, 185–195.

(7) Huang, W.; Manglik, A.; Venkatakrishnan, A. J.; Laeremans, T.; Feinberg, E. N.; Sanborn, A. L.; Kato, H. E.; Livingston, K. E.; Thorsen, T. S.; Kling, R. C.; Granier, S.; Gmeiner, P.; Husbands, S. M.; Traynor, J. R.; Weis, W. I.; Steyaert, J.; Dror, R. O.; Kobilka, B. K. Structural Insights into μ-Opioid Receptor

Activation. *Nature* **2015**, *524* (7565), 315-321.

(8) Dror, R. O.; Mildorf, T. J.; Hilger, D.; Manglik, A.; Borhani, D. W.; Arlow, D. H.; Philippsen, A.; Villanueva, N.; Yang, Z.; Lerch, M. T.; Hubbell, W. L.; Kobilka, B. K.; Sunahara, R. K.; Shaw, D. E. Structural Basis for Nucleotide Exchange in Heterotrimeric G Proteins. *Science (80-.).* **2015**, *348* (6241), 1361–1365.

(9) Koehl, A.; Hu, H.; Maeda, S.; Zhang, Y.; Qu, Q.; Paggi, J. M.; Latorraca, N. R.; Hilger, D.; Dawson, R.; Matile, H.; Schertler, G. F. X.; Granier, S.; Weis, W. I.; Dror, R. O.; Manglik, A.; Skiniotis, G.; Kobilka, B. K. Structure of the M-Opioid Receptor–Gi Protein Complex. *Nature* **2018**, *558* (7711), 547–552.

(10) Maeda, S.; Koehl, A.; Matile, H.; Hu, H.; Hilger, D.; Schertler, G. F. X.; Manglik, A.; Skiniotis, G.; Dawson, R. J. P.; Kobilka, B. K. Development of an Antibody Fragment That Stabilizes GPCR/G-Protein Complexes. *Nat. Commun. 2018 91* **2018**, *9* (1), 1–9.

(11) Schorb, M.; Haberbosch, I.; Hagen, W. J. H.; Schwab, Y.; Mastronarde, D. N. Software Tools for Automated Transmission Electron Microscopy. *Nat. Methods 2019 166* **2019**, *16* (6), 471–477.

(12) Zivanov, J.; Nakane, T.; Forsberg, B. O.; Kimanius, D.; Hagen, W. J. H.; Lindahl, E.; Scheres, S. H. W. New Tools for Automated High-Resolution Cryo-EM Structure Determination in RELION-3. *Elife* **2018**, *7*.

(13) Rohou, A.; Grigorieff, N. CTFFIND4: Fast and Accurate Defocus Estimation from Electron Micrographs. *J. Struct. Biol.* **2015**, *192* (2), 216.

(14) Adams, P. D.; Afonine, P. V.; Bunkóczi, G.; Chen, V. B.; Davis, I. W.; Echols, N.; Headd, J. J.; Hung, L. W.; Kapral, G. J.; Grosse-Kunstleve, R. W.; McCoy, A. J.; Moriarty, N. W.; Oeffner, R.; Read, R. J.; Richardson, D. C.; Richardson, J. S.; Terwilliger, T. C.; Zwart, P. H. PHENIX: A Comprehensive Python-Based System for Macromolecular Structure Solution. *Acta Crystallogr. Sect. D Biol. Crystallogr.* **2010**, *66* (Pt 2), 213.

(15) Pettersen, E. F.; Goddard, T. D.; Huang, C. C.; Couch, G. S.; Greenblatt, D. M.; Meng, E. C.; Ferrin, T. E. UCSF Chimera—A Visualization System for Exploratory Research and Analysis. *J. Comput. Chem.* **2004**, *25* (13), 1605–1612.

(16) Emsley, P.; Lohkamp, B.; Scott, W. G.; Cowtan, K. Features and Development of Coot. *Acta Crystallogr. Sect. D Biol. Crystallogr.* **2010**, *66* (Pt 4), 486.

(17) Robertson, M. J.; van Zundert, G. C. P.; Borrelli, K.; Skiniotis, G. GemSpot: A Pipeline for Robust

Modeling of Ligands into Cryo-EM Maps. *Structure* **2020**, *28* (6), 707-716.e3.

(18) Lee, J.; Cheng, X.; Swails, J. M.; Yeom, M. S.; Eastman, P. K.; Lemkul, J. A.; Wei, S.; Buckner, J.; Jeong, J. C.; Qi, Y.; Jo, S.; Pande, V. S.; Case, D. A.; Brooks, C. L.; III; MacKerell, A. D.; Jr.; … Im, W. CHARMM-GUI Input Generator for NAMD, GROMACS, AMBER,OpenMM, and CHARMM/OpenMM Simulations Using the CHARMM36 Additive Field. *J. Chem. Theory Comput.* **2016**, *12* (1), 405.

(19) Kilkenny, C.; Browne, W. J.; Cuthill, I. C.; Emerson, M.; Altman, D. G. Improving Bioscience Research Reporting: The ARRIVE Guidelines for Reporting Animal Research. *PLoS Biol.* **2010**, *8* (6).

(20) Wilson, L. L.; Alleyne, A. R.; Eans, S. O.; Cirino, T. J.; Stacy, H. M.; Mottinelli, M.; Intagliata, S.; McCurdy, C. R.; McLaughlin, J. P. Characterization of CM-398, a Novel Selective Sigma-2 Receptor Ligand, as a Potential Therapeutic for Neuropathic Pain. *Molecules* **2022**, *27* (11), 3617.

(21) Uprety, R.; Che, T.; Zaidi, S. A.; Grinnell, S. G.; Varga, B. R.; Faouzi, A.; Slocum, S. T.; Allaoa, A.; Varadi, A.; Nelson, M.; Bernhard, S. M.; Kulko, E.; LeRouzic, V.; Eans, S. O.; Simons, C. A.; Hunkele, A.; Subrath, J.; … Majumdar, S. Controlling Opioid Receptor Functional Selectivity by Targeting Distinct Subpockets of the Orthosteric Site. *Elife* **2021**, *10*, e56519.

(22) Váradi, A.; Marrone, G. F.; Eans, S. O.; Ganno, M. L.; Subrath, J. J.; Le Rouzic, V.; Hunkele, A.; Pasternak, G. W.; McLaughlin, J. P.; Majumdar, S. Synthesis and Characterization of a Dual Kappa-Delta Opioid Receptor Agonist Analgesic Blocking Cocaine Reward Behavior. *ACS Chem. Neurosci.* **2015**, *6* (11), 1813–1824.

(23) Chakraborty, S.; Uprety, R.; Slocum, S. T.; Irie, T.; Le Rouzic, V.; Li, X.; Wilson, L. L.; Scouller, B.; Alder, A. F.; Kruegel, A. C.; Ansonoff, M.; Varadi, A.; Eans, S. O.; Hunkele, A.; Allaoa, A.; Kalra, S.; Xu, J.; … Majumdar, S. Oxidative Metabolism as a Modulator of Kratom's Biological Actions. *J. Med. Chem.* **2021**, *64* (22), 16553–16572.

(24) Cirino, T. J.; Eans, S. O.; Medina, J. M.; Wilson, L. L.; Mottinelli, M.; Intagliata, S.; Mccurdy, C. R.; Mclaughlin, J. P. Characterization of Sigma 1 Receptor Antagonist CM-304 and Its Analog, AZ-66: Novel Therapeutics Against Allodynia and Induced Pain. *Front. Pharmacol* **2019**, *10*, 678.

(25) Hummel, M.; Lu, P.; Cummons, T. A.; Whiteside, G. T. The Persistence of a Long-Term Negative Affective State Following the Induction of Either Acute or Chronic Pain. *Pain* **2008**, *140* (3), 436–445.

(26) Salte, K.; Lea, G.; Franek, M.; Vaculin, S. Baclofen Reversed Thermal Place Preference in Rats with

Chronic Constriction Injury. *Physiol. Res.* **2016**, *65* (2), 349–355.